AJNR

Diffusion-Weighted MR Imaging Findings of Acute Necrotizing Encephalopathy

Sait Albayram, Zekeriya Bilgi, Hakan Selcuk, Dogan Selcuk, Halit Çam, Naci Koçer and Civan Islak

AJNR Am J Neuroradiol 2004, 25 (5) 792-797
http://www.ajnr.org/content/25/5/792

AJNR Am J Neuroradiol 25:792–797, May 2004

Case Report

Diffusion-Weighted MR Imaging Findings of Acute Necrotizing Encephalopathy

Sait Albayram, Zekeriya Bilgi, Hakan Selcuk, Dogan Selcuk, Halit Çam, Naci Koçer, and Civan Islak

Summary: Multiple, symmetrical brain lesions affecting the bilateral thalami and cerebral white matter, which often show a concentric structure on CT and MR images, characterize acute necrotizing encephalopathy (ANE) of childhood. We describe the imaging findings of a 2-year-old child with ANE obtained with diffusion-weighted MR imaging. We discuss the significance of these findings, as well as the pathophysiology of ANE lesions, with reference to the appearance of the disease as revealed by diffusion-weighted MR imaging.

Acute necrotizing encephalopathy (ANE) is a rare but deadly disease that is most prevalent in East Asia, but has also been identified in other parts of the world. Clinically, the disease is highly fulminant, with a rapid loss of consciousness, variable degrees of hepatic dysfunction, high mortality rates, and severe neurologic sequelae affecting its survivors (1–4). ANE also has a characteristic appearance on symmetric MR images: multiple lesions affecting the thalamus, deep periventricular white matter, putamina, cerebellum, and brain stem are visible on MR images of patients with ANE (1–7).

In the following report, we describe the diffusion-weighted and conventional MR imaging findings of a 2-year-old child with ANE. We discuss the significance of these findings, as well as the pathophysiology of ANE lesions, with reference to the appearance of the disease as revealed by diffusion-weighted MR imaging.

Case History

A 2-year-old girl presented with prolonged fever (72-hour duration) and vomiting (24-hour duration). She had not been given any aspirin. Physical examination of the patient revealed a fever of 40°C and signs of upper respiratory tract infection. Her liver was palpable 2 cm below the costal margins, arterial tension was 90/50 mm Hg, and heart rate was 140 beats per minute. Neurologic examination indicated a state of stupor; however, no evidence of meningeal irritation was found. Several hours after admission, the patient lapsed into a coma, becoming unresponsive to verbal commands and painful stimuli. There were hyperactive deep tendon reflexes, and she assumed a decerebrate posture. The initial diagnosis of the patient was encephalitis secondary to a viral agent. Intravenous acyclovir was administered to the patient for 5 days, followed by one dose of fresh frozen plasma and a vitamin K injection. A high dose of methyl prednisolone was administered for 3 days, followed by a course of dexamethasone for 10 days. L-carnitine, thiamine, pyridoxine, and biothine were administered for metabolic supplementation. A follow-up MR brain examination was performed on the 25th day of the patient's hospital admission. Laboratory tests revealed the aspartate transaminases and alanine transaminases levels were increased, measuring 3010 and 4750 IU/L, respectively. Hypoprotrombinemia was initially indicated by prothrombin activity level of 39%; however, this resolved after the patient received the plasma infusion and vitamin K injection. On examination, CSF was normal (no leukocytes, protein level of 15 mg/dL) except for mildly elevated pressure. Although throat-swab specimens did not reveal any evidence of influenza A, parainfluenza, or adenovirus antigen, the patient's serum influenza A antibody titer increased from less than 32 as measured on the 3rd day of her hospitalization to 1024 on the 12th day of hospitalization, indicating a recent influenza A infection. Percutaneous liver biopsy was performed to rule out metabolic or toxic liver diseases; the biopsy did reveal tissue changes secondary to hypoxia and perfusion defects. No fatty degeneration, as is consistent with Reye syndrome, was present.

A cranial MR examination was performed on the patient's 2nd day of hospital admission, during the most acute phase of illness (Fig 1A–C). Three distinct patterns on the thalamus and the deep cerebral white matter were visible on diffusion-weighted images (Fig 2A–C). The center of the lesions had higher apparent diffusion coefficient (ADC; 114×10^{-3} mm/s) values than the normal parenchyma, and very low ADC values (47×10^{-3} mm/s) were detected on the periphery of the central lesions (regions displaying ringlike enhancement) as is consistent with acute cerebral infarction. The outside portions of the thalamic and cerebral white matter lesions had high ADC values (136×10^{-3} mm three/s) consistent with vasogenic edema. On diffusion-weighted images, the central core of the pontine tegmenta, the cerebellar deep white matter, the upper part of vermis, both edges of the splenium of corpus callosum, and the deep cerebral white matter demonstrated low ADC values, consistent with acute cerebral infarction. The peripheral portions of these lesions registered high ADC values characteristic of vasogenic edema. On the basis of the MR findings, clinical presentation, and laboratory data, the diagnosis of acute necrotizing encephalopathy secondary to an influenza A viral agent was established. The patient's condition was critical for 3 weeks, after which time she began to improve slowly. MR images of the patient's brain obtained on the 25th day of her hospitalization revealed dramatic changes (Fig 3A–C). Although her condition improved somewhat, the patient never attained her premorbid level of consciousness or neurologic function. She was comatose for 20 days and exhibited no response to verbal commands or painful stimuli. On her 30th day of hospitalization, the patient's consciousness improved minimally. She is currently living with a severe neurologic disability as a result of her illness.

Received June 13, 2003; accepted after revision July 15.

From the Department of Radiology, Division of Neuroradiology (S.A., H.S., D.S., N.K., C.I.), and the Department of Pediatrics (Z.B., H.C.), Cerrahpasa Medical School, Istanbul University, Istanbul, Turkey.

Address correspondence to Sait Albayram, MD, Department of Radiology, Division of Neuroradiology, Cerrahpasa Medical School, Istanbul University, 34300 KMP-Istanbul, Turkey.

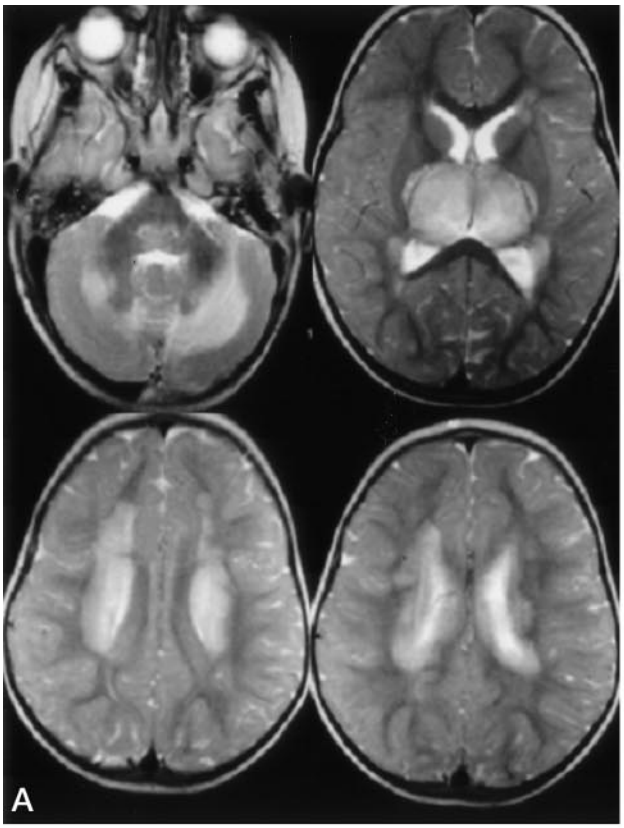

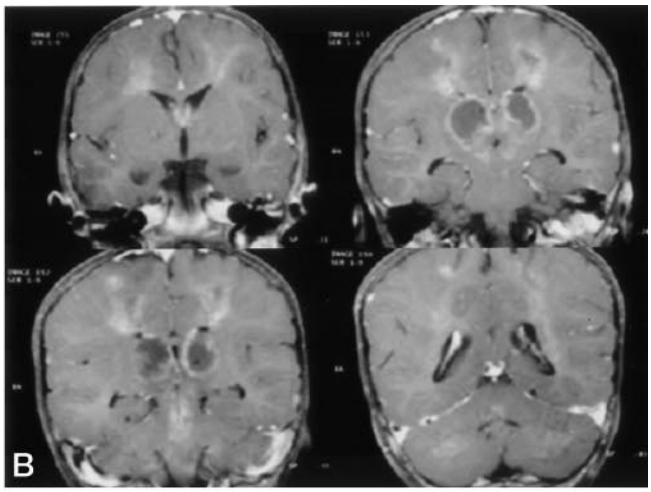

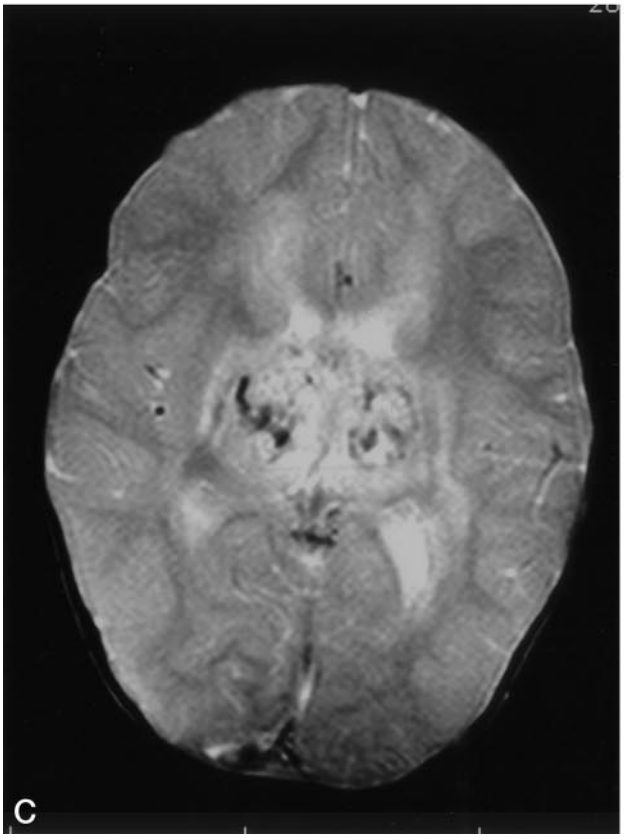

FIG 1. Conventional MR image findings in acute-stage ANE in 2-year-old-girl. *A,* Axial T2-weighted images show symmetric bilateral hyperintensities located deep in the cerebral-cerebellar white matter, bilateral thalami, and pontine tegmenta. *B,* Contrast-enhanced T1-weighted images reveal bilateral symmetric ringlike enhancement around the central hypointense portion of thalamic and central deep cerebral white matter lesions. Homogeneous enhancements in the pontine tegmenta and cerebellar white matter are also seen. *C,* T2-weighted gradient-echo MR image of the brain shows multiple, small hemorrhagic foci located on the central portion of thalamic lesions.

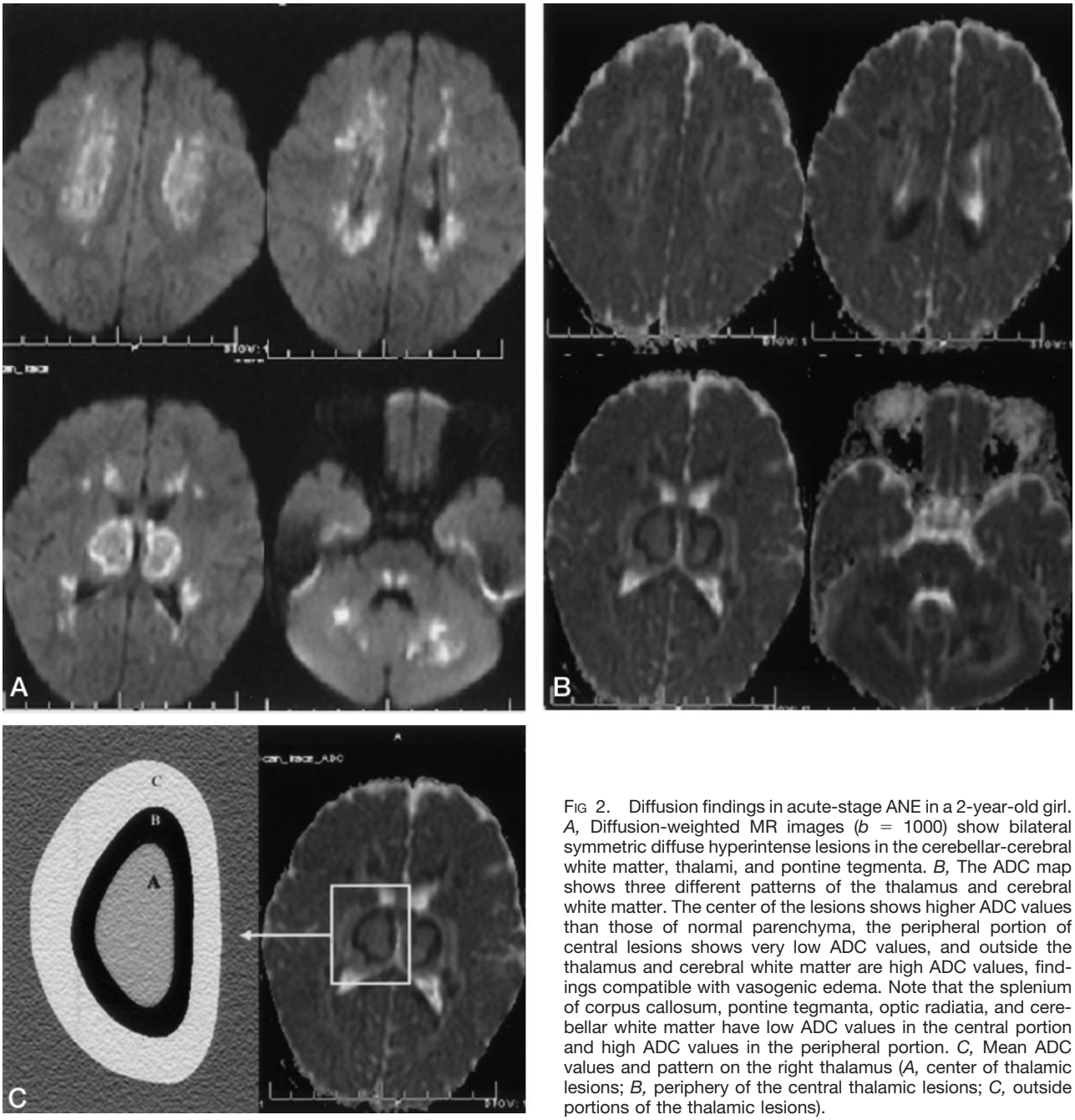

FIG 2. Diffusion findings in acute-stage ANE in a 2-year-old girl. *A,* Diffusion-weighted MR images (*b* = 1000) show bilateral symmetric diffuse hyperintense lesions in the cerebellar-cerebral white matter, thalami, and pontine tegmenta. *B,* The ADC map shows three different patterns of the thalamus and cerebral white matter. The center of the lesions shows higher ADC values than those of normal parenchyma, the peripheral portion of central lesions shows very low ADC values, and outside the thalamus and cerebral white matter are high ADC values, findings compatible with vasogenic edema. Note that the splenium of corpus callosum, pontine tegmanta, optic radiatia, and cerebellar white matter have low ADC values in the central portion and high ADC values in the peripheral portion. *C,* Mean ADC values and pattern on the right thalamus (*A,* center of thalamic lesions; *B,* periphery of the central thalamic lesions; *C,* outside portions of the thalamic lesions).

Discussion

Symmetrical, multifocal lesions are the most distinctive feature of ANE. The topographic distribution, as well as the progression, of these lesions is remarkably similar among patients of this disease. The thalamus is the structure most frequently affected by ANE, followed by the upper brain stem tegmentum, the cerebral white matter, and the cerebellar medulla. MR imaging and CT findings of ANE are well described in the literature (1–4, 8, 9). The literature also reports the use of angiography as an investigative tool during the acute phase of ANE (10, 11). Thus far, angiographic examinations of ANE patients have revealed neither stenosis of major arteries nor thrombosis of veins or dural sinuses. In one reported case, angiography revealed a reduction of blood flow within the posterior thalamoperforating, thalamogenuculate, and superior cerebellar arteries. In another reported case, stasis of the blood flow in the internal cerebral and Galen veins was visible on the angiographic examination. Oki et al (12) reported Technetium-99m ethylcyteinate dimer single-photon emission tomography (SPECT) findings that indicated marked hypoperfusion in thethalami appearing on the redistribution of delayed I [iodine 123]-iodoamphetamin SPECT images, which suggests that irreversible tissue damage had occurred despite recovery of blood flow within the thalami. Horada et al (13)

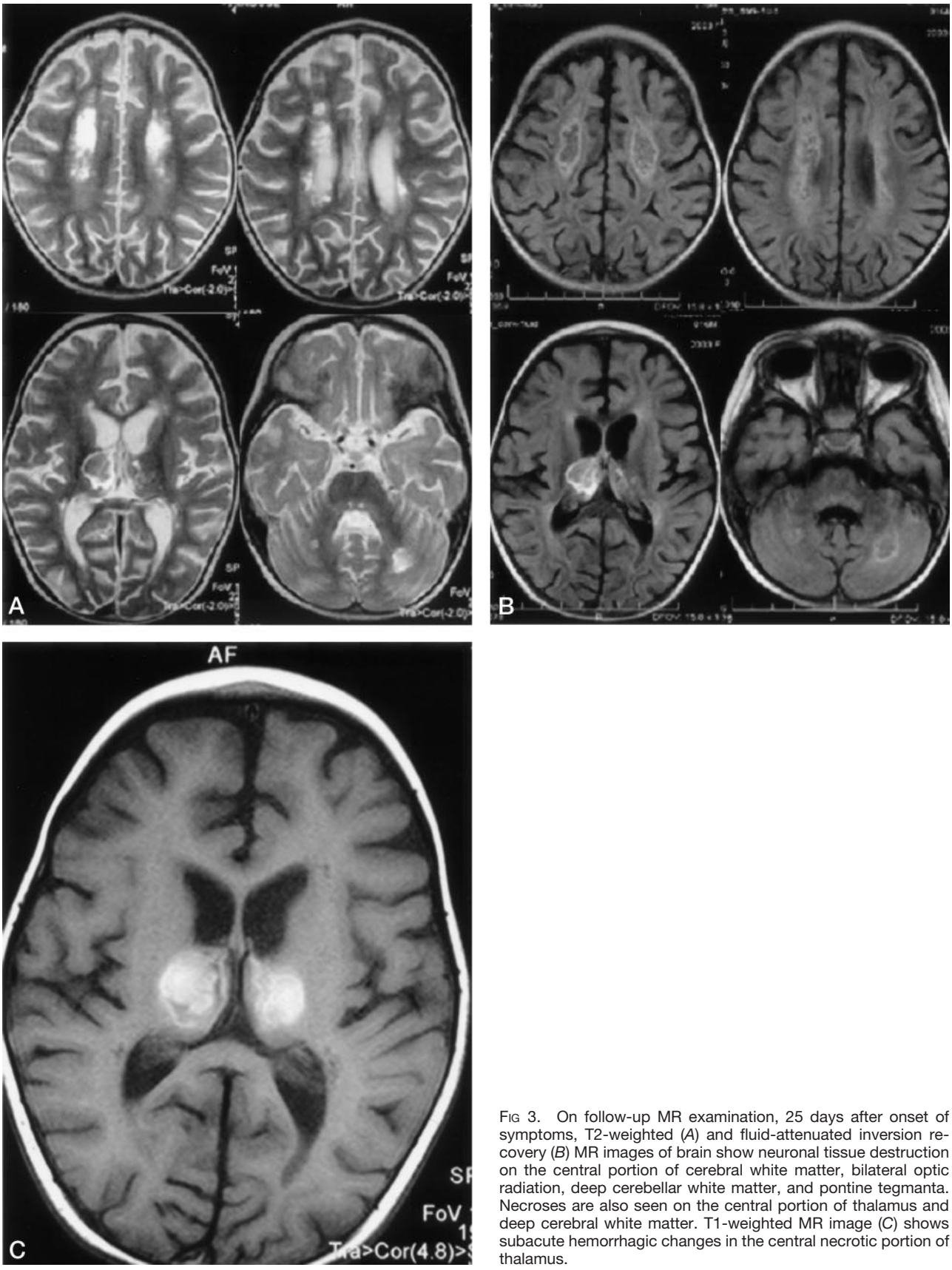

FIG 3. On follow-up MR examination, 25 days after onset of symptoms, T2-weighted (*A*) and fluid-attenuated inversion recovery (*B*) MR images of brain show neuronal tissue destruction on the central portion of cerebral white matter, bilateral optic radiation, deep cerebellar white matter, and pontine tegmanta. Necroses are also seen on the central portion of thalamus and deep cerebral white matter. T1-weighted MR image (*C*) shows subacute hemorrhagic changes in the central necrotic portion of thalamus.

briefly described diffusion-weighted images of an ANE patient in their case report comparing two different types of postinfectious encephalopathy: acute disseminated encephalomyelitis (ADEM) and ANE. Decreased ADC values were detected in ANE patients, but not in ADEM patients. This finding suggests that, as is also true in cases of acute cerebral infarction, cytotoxic edema is associated with ANE.

ANE and ADEM both occur after viral infections. The pathologic changes of ADEM have been well reported and the abnormality is shown mainly in the white matter. Histologically, ADEM is characterized by an acute perivenous lymphocytic inflammation with confluent demyelinetic lesions. By contrast, the exact pathogenesis of ANE is not yet well understood. Clinical and neuropathologic data suggest that a simple alteration of vessel wall permeability without disruption (mild cases) or vessel wall necrosis (severe cases) could be a possible phenomenon that initiates the reaction of the nervous tissue itself. The immediate results of such involvement may include vascular occlusion leading to neural tissue necrosis or transudation of serum with resulting perivascular and paranchymatous edema. These pathologic features indicate the vasogenic nature of edema and cytotoxic edema-necrosis in ANE resulting from local breakdown of the blood-brain barrier (1, 2, 5–7, 9). Why symmetrical, multifocal lesions are the most distinctive feature of ANE and the thalamus is the structure most frequently involved with ANE, followed by the upper brain stem tegmentum, the cerebral white matter, and the cerebellar medulla remains to be answered.

Neuropathologic data obtained from the autopsies of patients with ANE have been well described in the literature, enabling the interpretation of neuroimaging findings and providing insight into the pathogenesis of ANE lesions visible on radiographic examinations. During the acute phase, lesions in the thalamus, brain stem tegmentum, and cerebellar dentate nucleus are severely edematous, causing necrosis of involved nervous and glial cells. White matter lesions in the cerebrum and cerebellum are also edematous, with extravasation of a plasma-like substance without erytrocytes (1, 2). In their detailed account of the neuropathologic findings of ANE, Mizuguchi et al (2) observed that the center of the thalamic lesions showed perivascular hemorrhage and necrosis of neurons and glial cells. Examination of the periphery of the central portion of the thalamic lesions revealed congestion of arteries, veins, and capillaries and acute swelling of oligodendrocytes and progressive rarefaction of tissue. Extravasations around the artery and myelin pallor at the edge of thalamic lesion were also detected. Other than the thalamic lesions, superficial lesions within the deep white matter showed congestion of arteries and no abnormal paranchymal changes. In both gray and white matter lesions, no infiltration of inflammatory cells, except for a small number of extravasated leukocytes, was reported (2).

The ADC maps obtained from diffusion-weighted images of our patient reveal high ADC values in the center of the thalamic and deep cerebral white matter lesions. These ADC values, along with other MR findings, suggest necrosis within the deep cerebral white matter and hemorrhagic necrosis in the thalamus. The ADC values of the periphery of the central thalamic and deep cerebral white matter lesions were low, which suggests cytotoxic edema similar to the kind observed in acute cerebral infarction. Very high ADC values were detected in all of the peripheral portions of the pontine tegmenta and the cerebellar-cerebral white matter, the outside portions of the thalamic lesions, the upper part of vermis, and both edges of the splenium of corpus callosum, which suggests vasogenic edema. It is noteworthy that all areas of low ADC values showed prominent contrast enhancement on T1-weighted images that was compatible with breakdown of the blood-brain barrier. The follow-up MR imaging examination revealed that the center of the thalamic lesion showed a signal intensity pattern of subacute hemorrhage. In addition, all areas of low ADC values that enhanced with contrast material injection at initial MR imaging now had the appearance of subacute infarcts. All areas that had high ADC values on the initial MR imaging examinations revealed no lesions on the follow-up MR images.

The diffusion-weighted imaging features that we observed correlate well with the neuropathologic findings of ANE described by Mizuguchi et al (2). The inner core of the thalamus that showed high ADC values and hemorrhage could be explained as necrosis of neurons and glial cells. The very low ADC values of the periphery of the thalamic and deep cerebral white matter lesions that indicated cytotoxic edema could represent the acute swelling of oligodendrocytes and the progressive rarefaction of tissue. The high ADC value of the superficial lesions located outside the thalamus represents extravasations around the arteries and suggests vasogenic edema. The correlation of imaging and neuropathologic findings suggests that diffusion-weighted and MR imaging could be used both to determine the degree of neural destruction present in ANE patients and to predict the level of neuromotor skill that patients can expect to retain after the onset of the disease. As was shown by the follow-up MR examinations in the case presented here, high ADC values in the center of the thalamus or very low ADC values along the periphery of the thalamus during the acute phase or as revealed by contrast enhancement indicate necrosis or infarcted tissue, respectively. Our experience also showed that all portions of the brain (excluding central portions of lesions) showing high ADC values or nonenhanced lesions will resolve without resulting in destruction of the parenchyma.

On the basis of our experience with the patient described above and the imaging findings associated with her case, we conclude that diffusion-weighted imaging shows pathologic changes that differ from those shown by conventional MR imaging. In addition, these diffusion-weighted imaging findings correlate well with the known neuropathologic data asso-

ciated with ANE. During the acute phase of ANE, diffusion-weighted imaging may also be effective in predicting both the degree of neural destruction that will ultimately result from the disease and the level of neuromotor skill that can be expected.

References

1. Mizuguchi M. **Acute necrotizing encephalopathy of childhood: a novel form of acute encephalopathy prevalent in Japan and Taiwan.** *Brain Dev* 1997;19:81–92
2. Mizuguchi M, Hayashi M, Nakano I, et al. **Concentric structure of thalamic lesions in acute necrotizing encephalopathy.** *Neuroradiology* 2002;44:489–493
3. Shinjoh M, Bamba M, Jozaki K, et al. **Influenza A associated encephalopathy with bilateral thalamic necrosis in Japan.** *Clin Infect Dis* 2000;31:611–613
4. Sugaya N. **Influenza associated encephalopathy in Japan: pathogenesis and treatment.** *Pediatr Int* 2000;42:215–218
5. Mizuguchi M, Iia M, Takashima S. **Acute necrotizing encephalopathy of childhood: recent advances and future prospects.** *No To Hattatsu* 1998;30:189–196 (in Japanese)
6. Fujimoto Y, Shibata M, Tsuyuki M, et al. **Influenza A virus encephalopathy with symmetrical thalamic lesions.** *Eur J Pediatr* 2000;159:319–321
7. Nakai Y, Itoh M, Mizuguchi M, et al. **Apoptosis and microglial activation in influenza encephalopathy.** *Acta Neuropathol* 2003;105:233–239
8. Voudris KA, Skaardoutsou A, Haronitis I, et al. **Brain MRI findings in influenza A associated acute necrotizing encephalopathy of childhood.** *Eur J Paediatr Neurol* 2001;5:199–202
9. Yagishita A, Nakano I, Ushioda T, et al. **Acute encephalopathy with bilateral thalamotegmental involvement in infants and children: imaging and pathology findings.** *AJNR Am J Neuroradiol* 1995;16:439–447
10. Murakami Y, Iwata A, Hayakawa S, et al. **A case of acute necrotizing encephalopathy with low-density areas in the bilateral thalami on CT.** [In Japanese] *Nippon Shonika Gakkai Zasshi (Tokyo)* 1994;98:740–741
11. Momota K, Takashima Y, Maehara K, et al. **A case of acute necrotizing encephalopathy with low-density areas in the bilateral thalamus, cerebellum and periventricular region on cranial CT.** [In Japanese] *No To Hattatsu* 1989;21:271
12. Oki J, Yoshida H, Tokumitsu A, et al. **Serial neuroimages of acute necrotizing encephalopathy associated with human herpesvirus 6 infection.** *Brain Dev* 1995;17:356–359
13. Harada M, Hisaoka S, Mori K, et al. **Differences in water diffusion and lactate production in two different types of postinfectious encephalopathy.** *J Magn Reson Imaging* 2000;11:559–563